Laser Micro Machining for Continuous 3-D Contouring of Airflow Blades for a MEMS Turbine

Mark Heaton*

*Optical & Semiconductors Devices Group, Dept. of Electrical and Electronic Engineering
Imperial College London, Exhibition Rd, London SW7 2AZ,
E-mail: mark.heaton@imperial.ac.uk

This paper describes an innovative KrF excimer laser fabrication approach for profiling optimally smooth airflow contours. The research merit of the process is its use in producing a new type of electrical transducer micro-turbine using a novel axial format. [1] The necessary micro-machining precision for this was achieved by computer-controlling a laser beam using an elevating stage to step a moving mask across a fixed mask, i.e. a variant of dynamic mask-dragging or mask-aperturing. The moving mask image was projected on to a series of flat 600 μm wide, 1000 μm deep preform surfaces, reducing each to 50 μm thickness with curvature. Precise control of each mask increment to ablation depth and focus allowed a range of 3-D curves to be realized. The ablation rate versus surface quality was optimized throughout by ablating just 300 nm per laser pulse and using 2000 pulses spread over 90 sites. The process represents a cost effective means of using basic masks to continuously shape flat surfaces in the axial direction with high aspect ratios, high speed and precision, and is applicable to both micro streamlining and the manufacture of micro expansion nozzles.
DOI: 10.2961/jlmn.2007.03.0010
Keywords: 3-D, Excimer Laser Machining, Contouring, Micro, MEMS, Turbine Blades, SU-8

1. Introduction

The miniaturisation of electronic circuits well known in the micro electronics industry has been requiring similar downsizing in mechanical components and devices, particularly in the case of micro electromechanical systems, (i.e., MEMS). The aim of this paper is to show how laser machining can be computer controlled enough to fabricate curved 3-D micro-turbine blades from solid rectangular preform blades in the axial direction for a novel MEMS device. 3-D contouring in the axial direction of course involves controlling the laser beam in two directions (i.e., perpendicularly and laterally) as opposed to one direction if using the usual radial format (i.e., perpendicularly). This added complexity produces more sensitivity to low air-pressure when either measuring air/gas flow or producing power as the blade surface area is larger. [1] The fabrication technique differed from standard mask-dragging in that the laser beam area was set to vary in temperature along its longitudinal length in order to decrease each blade in thickness along its radial length.

The main rival 3-D contouring techniques applicable to SU-8 are based on building data contours in layers, e.g. the rapid prototyping techniques of parallel layering in stereolithography, laminated object manufacturing, selective laser sintering and fused deposition modelling. [2] These all tend to rely on complex slice algorithms and often acquire errors, holes, e.g. cracks and overlapping facets during the data entry stage regardless of the formatting file used, e.g. hewlett packard graphics language, and/or computerised topography. Another applicable method of depth contouring SU-8 is the multi-masked process of LIGA, (lithography electrodeposition). However, this process in addition to being slow requires both expensive complex masks and expensive access time to a synchrotron radiation source. [3] Perhaps the closest arrangement to that presented for 3-D laser ablation is the method of Half-tone masks. [4] These devices functioning as simple laser beam attenuators can, indeed, achieve 3-D contouring with depths of ~ 100 μm using 1000 laser pulses at 1 J/cm^2. However, their efficiency reduces when laser machining below ~ 100 μm due to thermal melting effects rather than laser ablation. MEMGen or EFAB metal layering technology using third-party 3-D CAD tools is also very useful for 3-D fabrication but takes weeks to produce even basic shapes and could not produce the geometries described using the laser machining techniques described in this paper [5].

The approach described in this paper thus has the novelty of achieving high resolution depth contouring using just two basic masks to aperture and selectively project a laser beam squarely across each blade's flat top surface in stages/pitches, decreasing or increasing in increments of parallel separation. The method at approximately one minute for the convex curve quadrant, and even less for the shorter inside concave curve, (a quarter section of a cambered cylindrical shell) is higher in speed to surface quality than comparable techniques over the same depth. [2 – 5] The system also utilizes refocusing for controlled profiling in confined spaces with minimal beam angle (5^o) taper (area reduction) and sidewall entrance ablation.

2. Find optimum laser fluence and depth per laser shot

In this paper a 248 nm excimer laser capable of a rep rate of 100 Hz at a pulse width of 23 ns at half max was used. This 248 nm wavelength laser offered high absorption and hence, depth per pulse/shot in SU-8 polymer and hence achieved smooth 3-D depth contouring. This wave-

length also being relatively short produces less beam spreading/divergence of the projected mask profile with increasing depth into the blade architecture. Deep Ultra Violet (i.e., UV) excimer lasers, unlike, e.g. CO_2/YAG types utilise primary photon electronic excitation, i.e. ablation rather than heat to issue material decomposition. The wavelengths 157-351 nm being those required to decompose the electronic bonds of most polymer plastics, e.g. SU-8, to a depth depending on the absorption of the beam in terms of pulse length to frequency.

Pulse lengths of ~ 8 ns at less than 1 J/cm^2, i.e. shorter than the surface heat diffusion time, are useful for welding/cutting etc., as the heat diffuses into the material during the pulse duration. However, energy diffusion from the ablation spot would be detrimental to this ablation process. The pulses for efficient depth and ablation need to be of an optimal frequency and fluence above ablation threshold. In other words, if the frequency is too high residual heat will not escape, and thermal effects such as wall angle slope taper due to melting will occur. [5] The effect of using an optimum fluence and frequency can be seen in the cross section photograph of a blade inlet wall in fig. 1, where the sidewall has sloped by only ~ 5^o. Such incoherent edge effects will be particularly acute in areas of long heat conduction time and residual heat isolation, e.g. in the corners where the blades join with the structural walls as seen later in fig. 8.

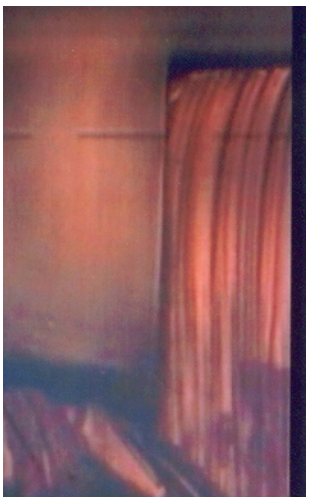

Fig. 1 Low inlet and sidewall angle drift; Laser ablation depth, 1000 µm

Thus, even if the pulse length and fluence are above ablation threshold for decomposition at the beam centre, melting/trenching may still occur at the edge walls. The effects of beam tapering (i.e., beam area reduction) as can be seen later in fig. 8, show blades ending in an undercut trench after tapering in slope by a best obtainable angle of ~ 5^o from the inlet side after 1000 µm of depth.

Wall angle tapering also arises with depth from progressive entrance ablation due to the laser beam entering at an angle from the -4x reduction lens. This was reduced by using low divergence optics of high NA, (i.e., numerical aperture) in addition to a high laser fluence to pulse rate. Air blowing (i.e., plume extraction) to remove the ablation products together with work stage elevations to maintain the focus at the same point after each ablation was also found to be effective in reducing such thermal effects. The optimum fluence for consistent ablation was found using the graph in fig. 2. Each point on this graph represents best-fit data from experiments in which a fixed number of shots were fired at SU-8 while increasing the fluence in increments. The ablation depth was measured using a Dektak 3ST (i.e., Sloan Technology) probe. As seen in fig. 2 the depth per shot gradually increased after a threshold fluence of ~ 0.1 J/cm^2, i.e. the minimum level required for ablation, below which the laser interaction will be thermal.

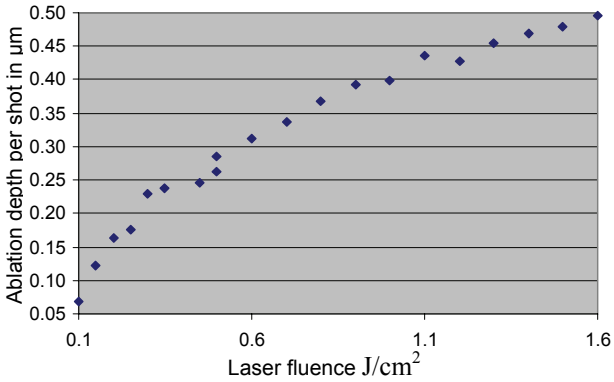

Fig. 2 Graph of depth per laser shot vs. fluence for SU-8

The laser fluence selected using the graph was such that the resultant ablation per shot could build up precise overall depth control to the required 600 µm depth and radius, R, with minimum beam angle taper and sidewall trenching (i.e., trench through-cut). The optimum decided fluence for consistent energy per pulse was ½ J cm^2 at a laser shot rate of 50 Hz, (i.e., a time period of 0.02 s) a level which in removing ~ ⅓ µm per shot could ablate the R 600 µm inside concave curve radius in 2000 shots, i.e. 50 each over a total of 40 steps of 15 µm in height.

2.1 Procedure for aligning the moving and fixed masks

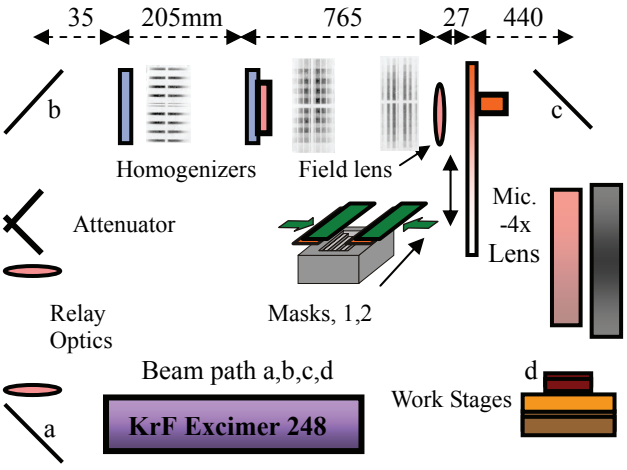

Fig. 3 Setup for laser contour depth micromachining

The beam path pointers a, b, c and d in fig 3 show the direction of the laser beam through the optics. The ho-

mogenizers were used to make more efficient use of the excimer's characteristic sharp peak output by acting to deconstruct and recombine the short and long optical axes respectively into a homogenised pattern having a flat Gaussian intensity cross section. The field lens projected a focused image of the moving mask (i.e., mask 2 on the z-axis elevator in fig. 3) above the entrance pupil of the reduction lens for focusing down to fit each blade's top surface area on the work stage. Next the reduction lens and microscope were set for mutual focus, i.e. the work stage elevation level where burns from the laser firing at 1 Hz produced a single sharp outline profile image of the moving mask on test sheets of Mylar polyester as seen in figs 4 and 5. Once a mutual focus for the microscope and reduction lens was determined, their offset coordinates were also found. Thus, any point located on the microscope would be as ablated under the -4x reduction lens.

The two masks used for all the depth profiling were both made under a microscope from tinplate strip sheets. The edges of the stationary mask were given a parallel separation of 3.78 mm, i.e. 1.15 mm wider than that of the 2.57 mm wide moving mask. The moving mask was of the critical dimensions needed in order to define an area of 615 x 1515 µm upon projection down onto each blade surface. The projected mask image exposed on the surface for ablation thus had enough clearance to maintain a size of at least 600 x 1500 µm after inevitable beam area reduction on ablating down to the full R 600 µm contour depth. The masks were separated by only 27 mm for minimal diffraction and arranged for either mutual upper or lower edge alignment by elevating the moving mask in steps of 0.1 and 0.01 mm, while stopping to fire static positioning shots at test Mylar.

The image burns were then observed on a microscope for the best parallax position, i.e. the fully open position with either the upper or lower edges of both masks just coinciding on the verge/periphery of cutting each other as seen in fig 4. Fig. 5 shows the effect of the masks beginning to close over each other. The image profile at this position should produce an image burn of 615 µm parallel separation, as would be expected if the fixed mask was omitted, i.e. no cutting of the beam passing through the moving mask.

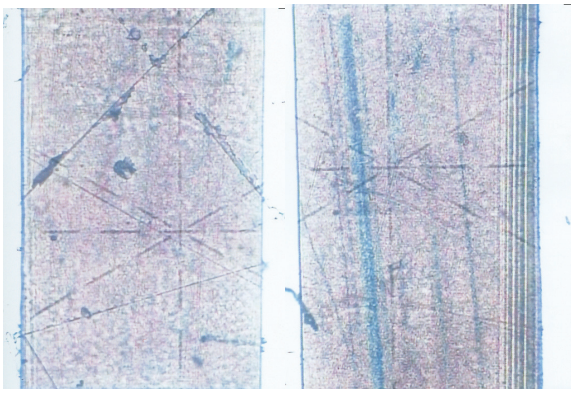

Fig. 4 Masks in focused, open and aligned position; Distance across; 615 µm

Fig. 5 Masks in focused, near open and aligned position

This separation was double checked by dividing the maximum open or closed separation for the masks by the -4 x beam reduction factor. The masks may need to be resized if due to optical losses the moving mask fails to ablate the required dimensions upon reduction. Once the moving mask was aligned it could be computer-controlled through 40 or 90 steps/pitches between 0 and 2.57 mm via lowering from mutual lower edge alignment for the clockwise stator blades, or elevating from mutual upper edge alignment to fabricate the rotor blades with mirroring slope to the stator blades.

2.2 Procedure for laser machining the concave inlets

The relative pitch lengths, X, for the inside concave curves are defined in Eq. 1 where $y = R/N$.

$$X = \frac{R}{N}\left(\sqrt{N^2-(n-1)^2}-\sqrt{N^2-n^2}\right) \qquad (1)$$

Thus R is the 600 µm contour radius and, N, the total number of pitches, i.e. 40, with n being a series of pitch closures 1 to 40. The contour depths were initiated by setting the laser to a repetition rate of 50 Hz and aligning it to fire 50 shots for the constant removal of 15 µm depths at ~ ⅓ µm per shot, under a fluence of ½ J/cm^2, with y = 600 µm/40, i.e. 15 µm. This ablation rate was maintained from the fully open mask position with refocusing after every ablation depth up until the last pitch before mask closure. The cumulative number of shots in all was 2000 for 40 steps ranging in length from 0.19 to 133.32 µm.

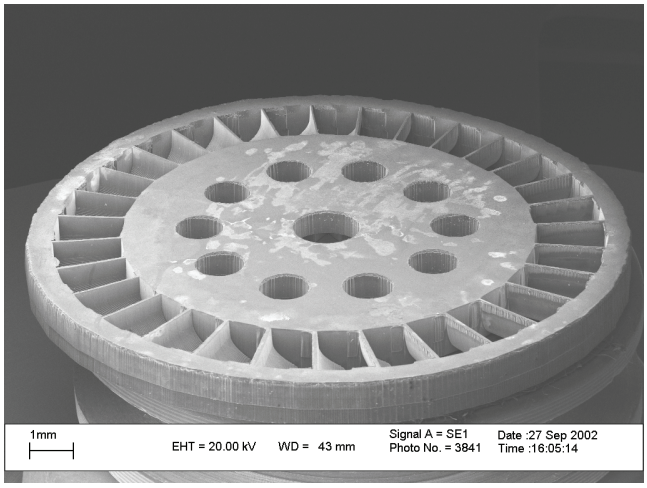

Fig. 6 Concave rotor blades showing leading-edge inlet walls

Using Eq. 1 for the convex curve, however, would produce an inherently large starting pitch of 133.32 µm. The inside concave in fig. 6 of course missed such steps as it commenced after the inlet wall, (tangential chord extension) as ablated by setting the laser to 1 J/cm^2 and firing 1700 shots at a rep rate of 20 Hz with the mask fully open. This, as can be seen earlier in fig. 1, shows the very good mark-to-space ratio obtained in that the sidewall angle has only increased to 5^o after 1000 µm of depth.

2.3 Procedure for laser machining convex contours

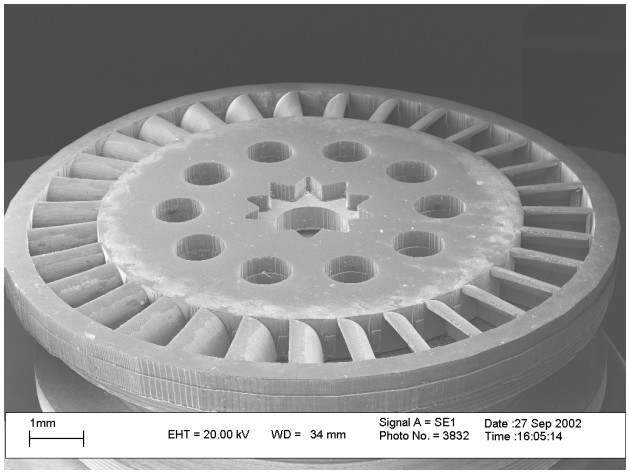

Fig. 7 Convex trailing outlet edges with bearing recess

The convex curves in fig. 7 were contoured to optimal smoothness by using 90 depth increments for 90 decreasing mask steps. The first layer/step was ablated with the mask fully open followed by a closure of X, before elevating up to maintain focus for the removal of the next layer. The lengths and depths of the steps follows from $\alpha = \pi/180$ and $\cos\alpha = d/R$. Each relative depth, d, may then be devised from Eq. 2 in terms of shots, with each subsequent depth subtracted from each previous depth to maintain the same relative focus height, where R gives an ablation depth of ~⅓ μm per shot at ½ J/cm^2.

$$d = R\left[\left(\cos(n-1)\pi/180\right) - \left(\cos n\pi/180\right)\right] \qquad (2)$$

Eq. 3 follows similarly for the mask step pitch lengths X, with each subsequent pitch subtracted from each previous one to maintain the correct relative position laterally across the blade surface of 600 μm absolute width.

$$X = R\left[\left(1-\sin(n-1)\pi/180\right) - \left(1-\sin n\pi/180\right)\right] \qquad (3)$$

3. Discussion of the contouring techniques and results

The profiles in figs 6 to 9 show remarkable contouring up to a final 50 μm thick inside trailing concave slope of $1:4/3$. This slope may be fine tuned if necessary by varying the shot number, and hence the inside curve radius. The final edge thickness midway along the blade chord length in fig. 8 was the best obtainable due to the unavoidable nature of heat conduction into the walls at the end corners of each blade. [6] Fabrication below 50 μm would result in blade fracture due to the decreasing linear radial thickness for constant airflow drag causing trench through-cut at the thinnest wall end-tips (i.e., points of maximum camber). The fine contouring mask stepping lines in fig. 9 for the convex may be further enhanced if required by doubling from 90, to 180 ½° steps.

Similarly, the surface quality of the inside concave in fig. 8 may be further enhanced by machining 120, 5 μm high steps instead of 40 at 15 μm. The extra time expenditure to surface quality would not, however, be justified in this instance unless conducive to increased mass airflow. The Reynolds number (i.e., inertial to viscous airflow force ratio) required in this instance was a relatively low ~ 3000 due to the airflow being only ~ 50m/sec. Using the two different techniques of constant depth to increasing length pitches, and gradually increasing depth to decreasing pitch steps, it was possible to optimize speed to surface quality for both blade surfaces overall.

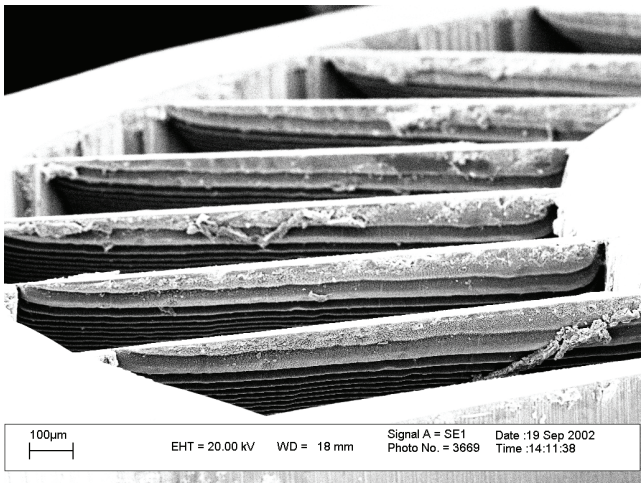

Fig. 8 Trailing blade edges with sidewall trenches and slope taper

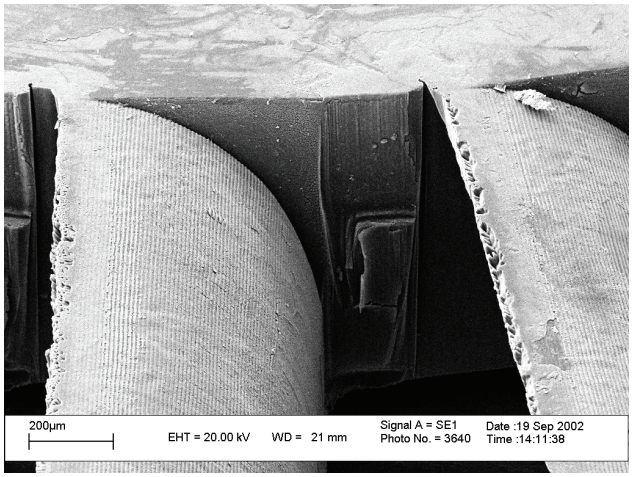

Fig. 9 Convex quadrant blade outlet using 90 ablation steps

A laser machining method using a basic computer-controlled moving mask closing in stages to both shield and admit a laser beam from a fixed mask has been presented as an effective means to smoothly contour an ideal micro-turbine blade surface in 3-D. The constant thickness and camber may be altered for other processes by using alternative pitch and depth values to those produced using Eqs 1 – 3. Also, depending on the mask dimensions, the contour micromachining may be applied to nozzle edges or, indeed, any other areas needing very smooth curvature for improved micro-fluidic flow. The advantages of this proc-

ess and design methodology as described are thus its accessibility to the multidimensional microstructuring of MEMS inserts, followed by high fabrication rates, flexibility and production-worthiness for mass production. The process also in using inexpensive basic masks would be very applicable where only a relatively small number of components needed to be fabricated or processed.

This research has thus made possible a truly 3-D microdevice design which would have otherwise been cumbersome, severely constrained and impractical to produce. The ability to create arbitrary complex 3-D geometries (i.e., continuous contour machining in the axial direction with a thickness variation in the radial direction) using precise ablation steps ranging from 300 nm has thus been met by the precision laser micromachining techniques described in this paper.

Acknowledgments

This work was supported by the EPSRC, under Grant No. GR/N18895. The author would like to thank Oerlikon for access to their KrF Excimer 248 laser workstation (model LPX 200).

References

[1] Holmes A.S., Hong G., Pullen K.R., Buffard K.R., Ax ial-flow Micro-turbine with electromagnetic generator: design, CFD Simulation and Prototype demonstration" MEMS Processing Symposium, 2004, 17th IEEE In ternational Conference on MEMS, Maastricht, The Netherlands, 25-29 Jan 568-571 (2004)

[2] Dr X. Chen, 'Direct slicing from power shape models for rapid prototyping', Int. journal for advanced manu facturing tech., 17:543-547, 2001.

[3] Marc J. Madou, Fundamentals of micro fabrication, Boca Raton, FL: CRC Press, Inc., ISBN 0-8493-9451-1, Ch. 6, Liga, pp. 275-279

[4] Holmes A.S., "Excimer laser micromachining with halftone masks for the fabrication of 3-D microstruc tures," IEE Processing on Science, Technology and Measurement 151, 85-92 (2004)

[5] www.MEMgen.com; website with high-tech layering methods for fabricating 3-D structures.

[6] Clark-MXR, Inc. – Ch. 3, Micromachining Handbook, pp. 2-3, http:///64.227.154.50 /Industrial /Handbook/ Chapter3.ht

(Received: June 20, 2007, Accepted: October 4, 2007)